9-5554-WRB93-012

Final Report of the Coherent Transient Systems Evaluation

F49620-91-C-0088

Wm. Randall Babbitt

Boeing Defense & Space Group

1993

Air Force Office of Scientific Research

REPORT DOCUMENTATION PAGE

Form Approved
OMB No. 0704-0188

1. AGENCY USE ONLY (Leave blank)	2. REPORT DATE	3. REPORT TYPE AND DATES COVERED
	17 Jun 1993	Final Report: 1 Sep 91 - 7 Jun 93

4. TITLE AND SUBTITLE
Final Report on the
Coherent Transients Systems Evaluation

5. FUNDING NUMBERS
Contract
F49620-91-C-0088

6. AUTHOR(S)
Dr. Wm. Randall Babbitt

7. PERFORMING ORGANIZATION NAME(S) AND ADDRESS(ES)
Boeing Defense & Space Group
P.O. Box 3999 7J-91
Seattle, WA 98124-2499

8. PERFORMING ORGANIZATION REPORT NUMBER
9-5554-WRB93-012

9. SPONSORING/MONITORING AGENCY NAME(S) AND ADDRESS(ES)
Air Force Office of Scientific Research /NE
Building 410
Bolling AFB DC 20332-6448

10. SPONSORING/MONITORING AGENCY REPORT NUMBER
2305/D5

11. SUPPLEMENTARY NOTES

12a. DISTRIBUTION/AVAILABILITY STATEMENT
unlimited

12b. DISTRIBUTION CODE

13. ABSTRACT *(Maximum 200 words)*

This final report of contract F49620-91-C-0088 describes the development of the analytical tools required to evaluate optical coherent transient memory, triple-product correlator, and continuous signal processor systems. One key tool is a coherent transient simulator based on the optical Bloch equations. The coherent transient output signal that results from an arbitrary sequence of pulses, each having an arbitrary amplitude, duration, center frequency, chirp, phase, and timing can be calculated. The simulator was used to study excitation pulse saturation and it effects on the output signal efficiency and fidelity and to study frequency chirped reference pulse saturation. Analytical tools were developed to assess the effects of local heating and spatial crosstalk. A performance evaluation of a coherent transient continuous optical correlator is reported, along with new implementation techniques. The continuous processor's predicted time-bandwidth product, data bandwidth, and pattern storage density are 10000, 5 GHz, and 100000 patterns per square centimeter, respectively. A proof of concept demonstration of the continuous optical processor was performed in europium doped yttrium silicate in collaboration with IBM Almaden Research Center. Research into divalent ion doped crystals as photon gated materials for coherent transient systems was performed.

14. SUBJECT TERMS	15. NUMBER OF PAGES
optical coherent transient, optical memories, triple-product correlator, continuous signal processor, optical Bloch equations, chirped reference pulses, photon gated materials	13
	16. PRICE CODE

17. SECURITY CLASSIFICATION OF REPORT	18. SECURITY CLASSIFICATION OF THIS PAGE	19. SECURITY CLASSIFICATION OF ABSTRACT	20. LIMITATION OF ABSTRACT
UNCLASSIFIED	UNCLASSIFIED	UNCLASSIFIED	UL

NSN 7540-01-280-5500

Standard Form 298 (Rev 2-89)
Prescribed by ANSI Std 239-18
298-102

INTRODUCTION

Real-time, wideband information storage and signal processing devices are critical to many military and commercial systems in order to perform complex functions such as secure communications, electronic surveillance and tracking, target recognition, tactical database management, and tactical air reconnaissance. Coherent transient optical memories and optical signal processors have been proposed as technologies capable of performing the above functions at data rates in excess of 10 GHz and with storage densities on the order of 10^{11} bits/cm^2. Initial calculations indicate that at moderate optical input power levels, the output signals would have sufficiently high signal to noise ratios to achieve reliable recall of stored/processed information. However, these calculations are solely based on a shot noise limited model and ignore the non-ideal properties of the medium, nonlinear effects, spatial crosstalk, gating efficiencies, local heating, the effects of non-ideal write and read pulses, and the characteristics of the light source, the modulation technique, and the detector. Compatibility and interfacing issues have not yet been addressed.

A major obstacle to realizing coherent transient based devices is the availability of suitable materials. There are several characteristics (broad inhomogeneous linewidth, narrow homogeneous linewidth, long storage times, operation and/or storage at elevated temperatures(>77 K), effectively singlet ground states, gateable storage with high efficiency, and high optical quality) that a storage material must possess before coherent transient memories and signal processors become practical. The absolute and relative importances of each these characteristics has yet to be examined.

The work performed under this contract addresses the above issues. The statement of work calls for the development of analytical tools which are needed to evaluate the performance of coherent transient memory and signal processing systems. The evaluations are then to be used to guide the development of coherent transient materials.

MODIFIED STATEMENT OF WORK

The contractor shall choose one coherent transient system and develop an appropriate system architecture. Candidate systems are a memory system, a triple product correlator, and a continuous optical correlator.

The contractor shall develop a set of analytical tools for evaluating coherent transient based systems. These tools will take into account the material properties, spatial crosstalk, the characteristics of the light source and the detector, and the detection and modulation schemes. The fidelity loss that can occur due to data pulse saturation and the effects of local heating of the material will be addressed. The system parameters to be determined include material thickness, spot sizes, laser powers, and output signal to noise ratios.

The contractor shall evaluate the chosen system architecture using expected performance characteristics for the individual components. The system performance characteristics include storage times, storage densities, access times, data bandwidths, time-bandwidth products, bit error rates, and processing accuracies. The contractor shall investigate the dependence of the systems' performance characteristics on the performance of the individual components. The contractor shall determine optimal values and tolerances for the system parameters that are variable and study the trade-offs between performance characteristics.

The contractor shall provide specifications for coherent transient materials in order to aid the development of materials that meet the requirements of the chosen coherent transient system.

The contractor shall characterize a candidate coherent transient material. Using the results of the material characterization, the contractor will provide guidance to improve the material growth.

If an appropriate material becomes available, the contractor will perform a proof of concept demonstration of a coherent transient system in a solid.

STATUS OF THE RESEARCH EFFORT

Previously Reported Progress

The work completed up to the end of 1992 was reported in the first annual report (see Appendix A).

Continuous Optical Correlator

A manuscript on the evaluation of the continuous optical correlator was submitted to Applied Optics. The submitted version is in appendix B. Since the annual report, the estimation of the performance of the continuous optical correlator was improved by including a maximum allowable non-linearity of the processor, homogeneous decay, and beam overlap efficiency. An optimal effective decay time of the excited state is derived. It was found that due to coupled effects, optimization of certain properties or efficiencies did not always yield optimal performance. Thus, the impact of each adjustable input parameters was carried through to the final result in order that full optimization of the pattern density could be achieved. The pattern density calculation was derived by evaluating the spatial crosstalk i the cases of 1) uncorrelated adjacent spots, 2) correlated adjacent spots, and 3) uncorrelated adjacent spots with a detection aperture.

Proof of concept demonstration of the Continuous Optical Correlator

In collaboration with Michael Jefferson and Miao Zhu at IBM Almaden Research Center, a proof of concept demonstration of the coherent transient continuous optical processor was performed in europium doped yttrium silicate. Though hyperfine split ground state transitions, like the $^7F_0$-$^5D_0$ of trivalent europium, are not ideal for continuous processing due to the fact that the single photon storage leads to destructive reads, they can be use for short term processing. A phase encoded 13-bit parker pattern was programmed into the

medium. The bit rate was 400 kHz. A 2.5 μsec reference pulse was used. After a 6 msec delay (the upper state lifetime is 2 msec), a stream of 1170 phase encoded bits was processed at the same 400 kHz bit rate. The duration of the data stream was thus 2.925 msec and longer than the upper state decay time and much longer than the coherence lifetime of the transition (roughly 600 μsec). The stream consisted of 9 repetitions of a 10-word sequence. The 10-word sequence was made up to 13-bit words. Six of the words in the 10-word sequence matched the 13-bit pattern pulse. Four of the words in the 10-word sequence were roughly orthogonal to the barker code and would not be expected to produce significant peaks when correlated with the pattern pulse. The resultant output signal would be expected to have 36 autocorrelation peaks that temporally coincide with the words that match the pattern pulse.

The experiment was performed at 2K. The isolation of the output signal from the "continuous" data stream was achieved by slightly angling the input beams. The data stream and output signal were simultaneously recorded on a digitizing oscilloscope. The problem of erasing the spectral gratings previously stored in the ground state hyperfine levels was done by ramping the beam power up and down while sweeping the laser frequency over the inhomogeneous bandwidth. After erasure, a single program and process experimental run was performed at one laser frequency setting and then the laser was tuned 1 MHz to a new "clean" area of the inhomogeneous bandwidth for the next experimental run. The term "clean" is relative, since a hole burned at one frequency creates hole and anti-holes over a 400 MHz bandwidth. Several experimental runs were performed. In over 90% of the runs, the resultant output signal was somewhat random. The reason for this is still under investigation, but could be due to excitation dependent dephasing, spectral diffusion, laser drift, or interference with previously recorded gratings. Despite this problem, several recordings of output signals were made in which all but one of the 36 autocorrelation peaks were well above the background and the last autocorrelation peak was present but comparable to the background. The autocorrelation peaks temporally corresponded to the words in the data stream that matched the pattern pulse.

Since the probability of such a output signal being generated randomly is less than one in 2^{1170}, the experiment provided a proof of concept demonstration of the coherent transient continuous optical processor.

Local Heating

The calculation of the effects of local heating in a cylindrically cooled medium were enhanced by deriving the equation for the temperature rise at the center of the optical beam rather than just at the edge. The effects of local heating on the performance of the continuous optical correlator were again found to be negligible.

Materials Research

The study of divalent samarium in potassium chloride was completed. The study revealed that at concentrations that were high enough to provide adequate absorption in a one centimeter long crystal the homogeneous linewidth of the $^7F_0$-$^5D_0$ transition was significantly broader than 100 MHz. The conclusion is that Sm:KCL is bad candidate for two-photon "gated" coherent transient materials. Research into divalent samarium doped into other hosts is incomplete and may produce better results.

Preliminary measurements on Tm:KCl revealed that the thulium concentration in the current sample (grown at the University of Utah) was lower than expected. Initial attempts to detect the florescence of the $^2F_{7/2}$ - $^2F_{5/2}$ transition produced a null result.

Our research into material system has found the following good candidate ions for photon gated coherent transient systems: Sm^{2+}, Tm^{2+} and Cr^{3+}. For the triple product correlator, a material system that is an ensemble of effective two-level absorbers is desirable. Effective two-level systems are also useful in experiments to verify aspects of the systems analysis. We have found the following good candidates ions for effective two-level systems: Tm^{2+}, Tm^{3+},

Sm^{2+}, Cr^{3+}, and Yb^{3+}. These ions are discussed below.

Divalent samarium $^7F_0 - ^5D_0$ *(689nm)* Divalent samarium is a promising effective two-level system and gated material since it does no exhibit nuclear hyperfine splitting and experiments demonstrating photon gate holeburning in Sm^{2+}:BaClF have been performed. The emphasis is on host systems with low symmetry that will yield higher oscillator strengths for divalent samarium and thus not require large concentration which lead to broadening of the homogeneous linewidth. For photon gating, sites capable of trapping 2+ and 3+ ions are needed. Hosts that shift the transition above 690nm are preferred in order to make the system more compatible with Ti:Sapphire lasers.

Divalent Thulium $^2F_{7/2} - ^2F_{5/2}$ *(1120nm)* The homogeneous linewidth and photoionization potential of divalent thulium has yet to be explored and it could prove to be a promising candidate material. For photon gating, the host crystal needs to have sites that are capable of trapping 2+ and 3+ ions. A host the shifted the transition below 1100 nm would be preferred to match the capabilities of Ti:Sapphire lasers.

Trivalent Chromium R lines (694nm) Photon gating has been demonstrated in Cr^{3+}:$SrTiO_3$. However, this crystal is cubic and the oscillator strength is very low. Chromium doped, non-centrosymmetric crystals that have sites capable of trapping 3+ and 4+ ions have the potential for high oscillator strength and high gating efficiency. Sufficiently high absorption coefficients can be obtained at concentration levels that don't induce significant spectral broadening provided a high magnetic field is applied to obtain long coherence times.

Trivalent thulium $^3F_4 - ^3H_6$ *(800nm)* The homogeneous linewidth of trivalent thulium is rumored to be very narrow. The transition wavelength is great for Ti:Sapphire and semiconductor lasers.

Trivalent ytterbium $^2F_{7/2} - ^2F_{5/2}$ *(1100nm)* The homogeneous linewidth of trivalent ytterbium has yet to be explored but has the potential to be quite narrow.

LIST OF PUBLICATIONS

A manuscript describing our results on the evaluation of the continuous optical correlator was submitted to Applied Optics. See appendix B.

PROFESSIONAL PERSONNEL

The bulk of the work was performed by Dr. W. Randall Babbitt. Dr. John A. Bell aided in the laser characterization of materials and in the evaluation of the continuous optical correlator. Dr. Bruce Evans has performed excitation and florescence studies of the Sm:KCl and Tm:KCl crystals. Dr. Evans and Dr. Rudy L. Prater have provided expertise on doped crystalline materials and the possible adaptation for coherent transients.

INTERACTIONS

Previously Reported Interactions

Interactions before December 1992 were reported in the first annual report (see Appendix A).

Joint Study Agreement with IBM

The joint study agreement between Boeing and IBM resulted in the proof of concept demonstration described above.

Appendix A

9-5554-WRB92-033

Annual Report of the Progress on the Coherent Transient Systems Evaluation

Wm. Randall Babbitt

Boeing Defense & Space Group

1992

Air Force Office of Scientific Research

INTRODUCTION

Real-time, wideband information storage and signal processing devices are critical to many military and commercial systems in order to perform complex functions such as secure communications, electronic surveillance and tracking, target recognition, tactical database management, and tactical air reconnaissance. Coherent transient optical memories and optical signal processors have been proposed as technologies capable of performing the above functions at data rates in excess of 10 GHz and with storage densities on the order of 10^{11} bits/cm^2. Initial calculations indicate that at moderate optical input power levels, the output signals would have sufficiently high signal to noise ratios to achieve reliable recall of stored/processed information. However, these calculations are solely based on a shot noise limited model and ignore the non-ideal properties of the medium, nonlinear effects, spatial crosstalk, gating efficiencies, local heating, the effects of non-ideal write and read pulses, and the characteristics of the light source, the modulation technique, and the detector. Compatibility and interfacing issues have not yet been addressed.

A major obstacle to realizing coherent transient based devices is the availability of suitable materials. There are several characteristics (broad inhomogeneous linewidth, narrow homogeneous linewidth, long storage times, operation and/or storage at elevated temperatures(>77 K), effectively singlet ground states, gateable storage with high efficiency, and high optical quality) that a storage material must possess before coherent transient memories and signal processors become practical. The absolute and relative importances of each these characteristics has yet to be examined.

The work performed under this contract addresses the above issues. The statement of work calls for the development of analytical tools which are needed to evaluate the performance of coherent transient memory and signal processing systems. The evaluations are then to be used to guide the development of coherent transient materials.

STATEMENT OF WORK

The contractor shall choose three coherent transient system architectures to evaluate. They include a memory system (either register, cache, RAM, mass, or archival storage), a triple product correlator, and a continuous optical correlator.

The contractor shall develop a set of analytical tools for evaluating coherent transient based systems. These tools will take into account the material properties, spatial crosstalk, the characteristics of the light source and the detector, and the detection and modulation schemes. The fidelity loss that can occur due to data pulse saturation, gating non-linearities, fine structure in the inhomogeneous profile, and reference and read pulse imperfections and the effects of local heating of the material will be addressed. The system parameters to be determined include material thickness, spot sizes, laser powers, and output signal to noise ratios.

The contractor shall evaluate the three chosen system architectures using expected performance characteristics for the individual components. The system performance characteristics include storage times, storage densities, access times, data bandwidths, time-bandwidth products, bit error rates, and processing accuracies. The contractor shall investigate the dependence of the systems' performance characteristics on the performance of the individual components. The contractor shall determine optimal values and tolerances for the system parameters that are variable and study the trade-offs between performance characteristics.

The contractor shall provide specifications for coherent transient materials in order to aid the development of materials that meet the requirements for coherent transient systems.

The contractor shall characterize materials provided by AFOSR. The materials are to be provided at no expense to Boeing. Along with the results of the materials characterization, guidance shall be provided in the growth of improved materials.

If an appropriate material becomes available, experiments shall be conducted to verify aspects of the system analysis and/or to perform a proof of concept demonstration of one of the coherent transient systems in a solid.

STATUS OF THE RESEARCH EFFORT

Coherent Transient Simulator

A key tool in our evaluation of coherent transient systems is a computer program that integrates the optical Bloch equations and follows the evolution of the density matrix elements during multiple excitation pulses. After the final excitation pulse, the density matrix elements contain the information necessary to calculate the resultant coherent transient response of the absorbing medium. Since the Bloch equations take into account nonlinear effects, the program is useful in studying the effect nonlinear excitation pulses. The program currently runs on a Macintosh IIci. It is written in C using console input (i.e. it is machine independent) and is thus directly portable to a PC-compatible, a workstation, or a mainframe computer. Eventually the computer program will be incorporated in the core of channel modelling programs used to evaluate the performance of memory and processing systems.

The Bloch equation integration program was originally developed at Boeing under Independent Research and Development funds. Under the current contract, several improvements have been made to the program that greatly enhance its speed, flexibility, and input and output capabilities. The exact analytical transformation of the density matrix elements resulting from excitation by a square pulse of arbitrary duration, amplitude, center frequency, phase, and timing was calculated and incorporated into the program. This greatly enhanced the programs speed since integrations of the matrix elements was no longer required. For example, the evaluation of the exact solutions of the Bloch equations for an excitation pulse sequence consisting of 32 square pulses for 1025 frequency points takes only 115 seconds on a Macintosh IIci. Chirped pulses of

arbitrary of arbitrary duration, bandwidth, amplitude, center frequency, phase, and timing are still calculated by integration of the optical Bloch equations. A typical chirps pulse requires about 2 minutes to calculate the resultant density matrix elements for 1025 frequency points with 1 part in a 1000 accuracy (7 minutes for 1 part in 10^9).

The improvements in input capabilities and calculation flexibility include options for 32-bit data pulses, gating pulse, sudden losses in coherence, and homogeneous decay Data pulse up to 32-bits long can be entered as a single integer and can be amplitude or phase encode, return to zero (RZ) or non-return to zero (NRZ). Data pulses longer than 32-bits are achieved by repeating this options indefinitely. The gating pulse option simulates the effects of a gating pulse by eliminating those atoms in the upper state at the time of the pulse, thus permanently modifying the inhomogeneous profile. The resultant modulations in the inhomogeneous profiles will alter the effect of excitation pulse nonlinearities compared to an unmodulated inhomogeneous profile. The ability to create a sudden loss of coherence aids in simulating absorbers with homogeneous decay times much shorter than the upper state lifetimes and in simulating the rejection of spurious outputs via spatial isolation (since the program does not do spatial integrations). Homogeneous decay can now be optionally included in the standard bloch equations for chirped or square pulses.

The output now include direct detection, coherent detection, and the resultant holeburning spectra. The graphical interface allows quick evaluation of the results. The interface in achieved via a different program that is simultaneously resident with the coherent transient simulator. This separation maintains the quick portability of the simulator to other machines.

Modified Bloch Equations

The implementation in the simulator of the modified Bloch equations which correct the failures of the ordinary Bloch equations to predict the effects of homogeneous decay during strong excitation pulses was considered. During

intense pulses, the dephasing time can be considerably longer than in the zero intensity limit in certain materials and under certain conditions. However, since the main concern for coherent transient memory and signal processing systems is the fidelity of the output signals which rely heavily on the materials response to the data pulses, it is the coherence decay during the data pulses that is of greatest concern. However, the spectrum of the data pulse is by necessity complex with regions of high and low spectral density. If the above phenomena were required to play a role, it would differentially affect the spectral components of the data pulses, resulting in a loss in output fidelity. There may be techniques that circumvent these problems or take advantage of this phenomenon in another way in order to increase storage densities or time-bandwidth products. However, it is not in the scope of this work to address these issues. Thus, only consider cases in which the intensity dependent homogeneous decay is relatively weak so that any lengthening of the dephasing time will not significantly alter the resultant output signals were considered.

Results Obtained With Simulator

The major result obtained so far with the simulator was the effect of saturation on chirped pulses when used as reference pulses in time domain memories. Previous analyses of chirped reference pulses have assumed that the medium responds linearly to the chirped reference pulses. However, to be efficient, reference pulses must be able to act as effective $\pi/2$ and π pulses. Reducing the amplitude of the reference pulses to the linear regime would reduce the output signal by three to four order of magnitude.

In studying the effects of chirped pulses as reference pulses, it is not sufficient to merely study the chirped pulses ability to invert 50% or 100% of the atoms. The effects of saturation on the coherences must be taken into account. Using the simulator, excitation pulse sequences that contained chirped reference pulses were compared to sequences with brief reference pulses. By optimizing the intensity of the chirped pulses, it was shown that chirped pulses are nearly as

intense pulses, the dephasing time can be considerably longer than in the zero intensity limit in certain materials and under certain conditions. However, since the main concern for coherent transient memory and signal processing systems is the fidelity of the output signals which rely heavily on the materials response to the data pulses, it is the coherence decay during the data pulses that is of greatest concern. However, the spectrum of the data pulse is by necessity complex with regions of high and low spectral density. If the above phenomena were required to play a role, it would differentially affect the spectral components of the data pulses, resulting in a loss in output fidelity. There may be techniques that circumvent these problems or take advantage of this phenomenon in another way in order to increase storage densities or time-bandwidth products. However, it is not in the scope of this work to address these issues. Thus, only consider cases in which the intensity dependent homogeneous decay is relatively weak so that any lengthening of the dephasing time will not significantly alter the resultant output signals were considered.

Results Obtained With Simulator

The major result obtained so far with the simulator was the effect of saturation on chirped pulses when used as reference pulses in time domain memories. Previous analyses of chirped reference pulses have assumed that the medium responds linearly to the chirped reference pulses. However, to be efficient, reference pulses must be able to act as effective $\pi/2$ and π pulses. Reducing the amplitude of the reference pulses to the linear regime would reduce the output signal by three to four order of magnitude.

In studying the effects of chirped pulses as reference pulses, it is not sufficient to merely study the chirped pulses ability to invert 50% or 100% of the atoms. The effects of saturation on the coherences must be taken into account. Using the simulator, excitation pulse sequences that contained chirped reference pulses were compared to sequences with brief reference pulses. By optimizing the intensity of the chirped pulses, it was shown that chirped pulses are nearly as

efficient as brief pulses in storing and recalling information. Another important criteria is the sideband noise introduced with chirped pulses of finite duration. Our results demonstrate that the sidebands drop off rapidly and will not lead to intersymbol interference that can degrade performance in memory or signal processing systems. These results are significant since sufficiently intense brief reference pulses are difficult to produce and chirped pulses present a practical alternative. A similar evaluation of saturation effects and efficiencies for phase encoded reference pulses is planned. Phase encoded reference pulses may have the disadvantage that they only work in the linear regime and thus lead to inefficient storage and recall.

For signal processing applications, coherent transients act as triple product correlators. If correlations between two signals is desired, the third pulse previously was required to be brief pulse. Unlike in memory applications were a matched pair of chirped pulses can replace the two brief reference pulses, in the processing case a single chirped pulse can not replace a brief pulse. However, a technique was discovered by which two chirped pulses can replace a single reference pulse and without any loss in efficiency. The chirped pulses are the first two pulses in a four pulse sequence. The last two pulses are the signals to be processed. The chirped pulses have the same chirp bandwidth, but the second pulse's chirp rate is twice that of the first pulse. Employing our simulator, it was found that optimization of the intensities of the chirped pulses produced output signals with the same efficiency as optimized brief pulses and with negligible intersymbol interference. This technique works for both the triple product correlator and the continuous optical correlator.

Continuous Optical Correlator

The performance of the continuous optical correlator was evaluated. In carrying out this evaluation, a technique (discussed above) was discovered for replacing a brief reference pulse with two chirped pulses. One difficulty with the continuous optical correlator is isolating the output signal from the continuous

input signal and from the numerous spurious echoes that are created. This is especially true when the brief reference pulse is replace by two chirped pulses. Polarization isolation is simple, but does not work well in practice with nonideal systems. Angular separation leads to a reduction in efficiency and presents technical alignment difficulties in a practical system. It was discovered that a simple counter-propagating configuration provides complete isolation from spurious coherent transient signal. Polarization isolation, though not required, can be added to eliminate any backscattered light and provide additional isolation.

The optimized performance of the continuous optical correlator was derived by balancing the coherent saturation intensity and incoherent saturation intensity and by balancing the spot size needed to maintained a required signal to noise with the diffraction limited spot size. The effects of local heating were calculated. The calculations confirmed that the effects were negligible in the cases studied. The analysis took into account the pattern write efficiencies, gating efficiencies, and the signal output efficiencies including input signal absorption and output signal gain in strongly absorbing media. The performance characteristics that were optimized in the evaluation are the time-bandwidth product of the correlator and the obtainable pattern storage density (number of patterns per unit area). Though the optimized results were obtain assuming the material parameters for Sm^{2+}:KCl, the calculations are applicable to any material. Using the current material parameters for Sm^{2+}:KCl, a time bandwidth products of 800 and a pattern density of 3000 per square centimeter is predicted. By assuming conservative estimates of the material parameters that could be obtained for Sm^{2+} in a similar hosts, it is predicted that a time bandwidth product of 16000 could be achieved with pattern density of 8×10^5 pattern per square centimeter. A paper was presented on these results and a manuscript is currently being prepared for publication (see below).

Local Heating

The effects of local heating on the performance of the continuous optical

correlator were calculated and found to be negligible. The processing medium was assumed to be cylindrical (1 cm in diameter) and cooled only on the circumference. However, for memory applications the sample area may be significantly larger and heat may need to be removed from the back and/or the front face of the sample. To handle these cases, A two dimensional thermal diffusion modelling program for axially symmetric samples was written.

Spatial crosstalk

In the results described above, in determining spatial densities the assumption was made that each pixel was isolated from its neighbors. This assumption is sufficiently valid for beams of finite extent (i.e. top hat shaped). In practice, the production of such beams is inefficient. Gaussian beams are efficiently produced but have infinite widths, though the intensity in the wings drops off dramatically. The maximum storage density depends on how closely the pixels can be located without degrading the information stored.

An equation for the coherent transient output signal produced when a gaussian recall pulse of arbitrary waist is an arbitrary distance from a pixel written with two or more gaussian pulses of arbitrary waist was derived. The calculation takes into account the full two dimensional, nonlinear overlap of the beams. It assumes a uniform waist throughout the length of the material. A calculation of the overlap in mediums where diffraction is significant is planned, followed by a study of the maximum storage density as a function of the tolerable crosstalk and of the ratio of the nearest neighbor distance to the spot size.

Coherent Transient Systems Evaluation

As discussed above, the performance of the continuous optical correlator has been evaluated using Sm:KCl as the processing medium. A more complete study of the trade-offs is to follow. During the evaluation of the continuous correlator, most of the analytical tools for evaluating the triple product correlator and memory systems were developed as well. However, evaluation of a practical and

competitive memory system requires knowledge of the techniques for obtaining densities far beyond the "isolated pixel" and "isolated bit" approach. A joint study agreement with IBM to explore these avenues together was signed. Their expertise in the area of optimization of memory channels will prove invaluable to this task.

Materials Research

Development of practical coherent transient memory and signal processing systems can not proceed without better materials. There are several material systems based on population storage in ground state hyperfine levels. These materials provide excellent demonstrations and can be used to confirm theoretical predictions. But, hyperfine materials have two disadvantages that make their use as practical materials improbable. The first disadvantage is the single photon writing process which leads to destructive readout. Minimizing the effects of the destructive readout requires lowering the writing efficiency or lowering the readout beam intensity. Both methods severely degrade the signal to noise. The second disadvantage is coherent beating. Since the hyperfine splittings are several order of magnitude less than the inhomogeneous linewidth which determines the ultimate data rate, attempts to use the full bandwidth leads to beating between the levels and severe modulation of the output signal.

For these reasons, two-photon "gated" coherent transient materials are being investigated. There has been some demonstrations of gated spectral holeburning materials, but the homogeneous linewidths of these materials make them impractical as coherent transient materials. One such material demonstration, using Sm^{2+}:BaClF, employed photoionization as the gating process, transforming Sm^{2+} to Sm^{3+}. The linewidth of the burned holes were 25 MHz. However, sub-megahertz linewidths have been noted in Sm^{2+}:KCl and photon gating should be possible after some modifications of the crystal. A grower of alkali halide materials, Matt DeLong at the University of Utah, is willing to grow experimental crystal at a very low cost (≈ $550 per crystal). Four crystals have

been grown to date. The first two exhibited very weak lines compared with earlier studies. This was probably due to possible contamination of the $SmCl_2$ used to grow the crystals. The second two crystals were grown with a new stock of $SmCl_3$ and a modified growth technique. Unlike the first two crystal, they have a deep purple color indicative of high Sm^{2+} concentration. Characterization of these latest materials had just started when our argon laser tube failed. The tube has just been replaced and characterization will continue at the first of the year.

LIST OF PUBLICATIONS

A manuscript is in preparation describing our results on the evaluation of the continuous optical correlator.

A paper on the saturation effects of chirped and phase encoded reference pulses is planned for submission in the next few month when the results on the phase encoded reference pulses is completed.

PROFESSIONAL PERSONNEL

The bulk of the work is being performed by Dr. W. Randall Babbitt. Dr. John A. Bell is aiding in the laser characterization of materials and the determination of performance criteria for signal processors. Dr. Bruce Evans has performed excitation and florescence studies of the Sm:KCl crystals. Dr. Evans and Dr. Rudy L. Prater have provided expertise on doped crystalline materials and possible their adaptation for coherent transients.

INTERACTIONS

Papers Presented

A paper was presented at the Spectral Hole-Burning and Luminescence Line

Narrowing: Science and Application conference in Ascona, Switzerland, September 14-18, 1992. The paper was entitled "Continuous Signal Processing Using Optical Coherent Transients" and described the evaluation of the performance of the continuous optical correlator, as discussed above.

PSHB workshop

A workshop was hosted at Boeing on persistent spectral holeburning. The participants were Randy Babbitt and Matt Derstine of the Boeing Company Yu Sheng Bai and Ravinder Kachru of SRI International, Alan Craig of AFOSR, Anshel Gorokhovsky of City College of CUNY, Philip Hemmer of ROME Air Dev. Ctr., Mike Jefferson and Roger M. Macfarlane of IBM Almaden Res. Ctr., M. K. (Paul) Kim of Wayne State University, Thomas W. Mossberg of the Univ. of Oregon. The topics discussed were hyperfine storage and beating, homogeneous linewidths, spectral diffusion, gated storage, novel storage concepts, competitive technologies, practical system considerations, current materials, sources of materials. A summary of the meeting was distributed.

Joint Study Agreement with IBM

A joint study agreement was signed between Boeing and IBM in November. Dr. Babbitt visited IBM for two weeks in December to discuss with Dr. Michael Jefferson the issues we are going to address jointly. Since a major part of the collaboration will include experimental work at IBM, the visit also enabled Dr. Babbitt to familiarize himself with IBM operations. He had the opportunity to help set-up Dr. Jefferson's new cryostat and the associated optics and electronics. Photon echoes, optical nutation, and hole-burning were obtained by the end of the visit.

Appendix B

Coherent Transient Continuous Optical Processor

Wm. Randall Babbitt and John A. Bell

Boeing Defense & Space Group

P.O.Box 3999 M/S 7J-91

Seattle, WA 98124-2499 USA

(206) 865-3307

ABSTRACT

After the absorption profile of an inhomogeneously broadened solid is programmed by two temporally modulated pulses (at least one encoded with a pattern), it can be gated to permanently fix the ground state spectral population distribution. The subsequent illumination of the solid by an uninterrupted, temporally modulated optical beam results in a coherent transient output signal that represents the correlation of the signal with the stored pattern. Multiple patterns can be stored at different locations on the sample and accessed randomly, enabling fast reprogramming of the processor. A performance analysis of this novel optical signal processor predicts that real-time continuous processing is possible with a processor bandwidth exceeding 5 GHz, a time-bandwidth product exceeding 10^4, and a pattern storage density exceeding 10^5 patterns per cm^2.

Keywords: optical coherent transients, photon echoes, spectral hole-burning, optical signal processing, optical correlator.

Note to Publisher (not to be included in manuscript)

This manuscript is submitted for publication with the understanding that the United States Government is authorized to reproduce and distribute reprints for governmental purposes.

1.0 Introduction

The continuous optical correlator presented here is based on the phenomena of coherent transients, also referred to as photon echoes or time-domain spectral holeburning. Long-term coherent transient storage of temporally modulated optical data pulses[1] in cryogenic solids has been demonstrated by several authors.[2,3,4] The temporally encoded information is stored as a spectral interference pattern in the ground or excited state inhomogeneously broadened population distribution. Permanent storage and non-destructive reading capabilities can be achieved via a gating process that permanently fixes the spectral population grating. Such processes have been demonstrated for frequency-domain spectral holeburning.[5] Optical coherent transient techniques can also be used to perform convolutions and correlations of three temporally modulated light pulses.[6] The coherent transient output signal represents the cross-correlation of the first pulse's temporal waveform with the convolution of the second and third pulses' waveforms. The processor responds to the electric field amplitudes of the input pulses and thus can fully process amplitude, phase, and frequency modulated signals.[7] In previously proposed implementations,[8] it has been asserted that to obtain high fidelity correlations, the durations of the modulated input pulses must be less than the homogeneous decay time of the absorbers. To search an uninterrupted data stream (data streams longer than the homogeneous decay time) for a given pattern requires that the signal be broken up into overlapping segments that must be processed separately. In order to process each segment, the optical pattern/reference pulses would have to be regenerated and introduced into the medium. Thus, three modulated light beams with appropriate delays need to be generated for each segment processed. The resultant signals would then have to be additionally processed to obtain the true correlation. These limitations greatly increase the processor's latency time and make real-time processing of continuous signals impossible.

In this paper, we introduce a novel coherent transient signal-processing technique that enables the real-time processing of continuous input signals after a single programming stage.[9] The unique features of the continuous optical correlator and the techniques for programming it and obtaining high fidelity correlation peaks are discussed. Then a more detailed analysis of the continuous processor's potential performance is presented. Data rates on the order of 10 GHz, time-bandwidth products up to 10^5, and pattern storage densities in excess of 10^5 patterns per cm^2 are predicted.

1.1 Coherent Transient Triple Product Correlator

Consider three temporally encoded light pulses. These light pulses may be amplitude, phase, and/or frequency encoded. When an inhomogeneously broadened absorber is resonantly excited by these pulses in sequence, the resultant coherent transient output signal $E_s(t)$ is given by[10]

$$E_s(t) \propto \int_{-\infty}^{\infty} d\tau'' \, E_1(\tau'') \int_{-\infty}^{\infty} d\tau' \, E_2(\tau') \, E_3(\tau'' + t - \tau') \quad , \qquad (1)$$

where $E_j(t)$ represent the electric field of the j^{th} pulse. The output signal represents the correlation of the first data pulses with the convolution of the second and third data pulses. Either the convolution or correlation of only two pulses can be achieved if one of the three data pulses has only a single subpulse whose duration is less than the shortest temporal feature of the other two pulses. The above equation for the output is valid regardless of the modulation characteristics of the data pulses. Thus, a coherent transient correlator is capable of simultaneously performing phase and frequency correlations, as well as amplitude correlations. The data bandwidth of the triple product correlator is ultimately limited by the inhomogeneous bandwidth of the absorbing transition. For such transitions in solids, data bandwidths can range from a gigahertz to a terahertz. The correlator's time-bandwidth product is limited by the ratio of the inhomogeneous to homogeneous broadening, which was measured to be as high as 10^7 in one solid.[11]

2.0 The Coherent Transient Continuous Optical Processor

The assertion made previously that all the pulses must be less than the homogeneous decay time is not valid in all cases. Though the time-bandwidth product is limited by the homogeneous dephasing time, the data pulse lengths are not. The duration of the third pulse is not even limited by the population decay time and can actually be infinite. To accomplish this improvement, a step must be added to the programming of the coherent transient correlator which permanently stores the ground state population grating produced by the first two data pulses. This step is referred to as the gating. The programming, gating, and processing stages of the coherent transient continuous optical correlator are illustrated in figure 1.

2.1 Programming and Gating the Continuous Processor

Programming the continuous processor is accomplished by illuminating the material with two modulated light pulses: a pattern pulse and a reference pulse. The effect of these first two pulses

is identical to the first two pulses in the triple product correlator in that the resultant frequency dependent population gratings in ground and excited states are equivalent. The next step is a gating process to prevent erasure of the ground state population distribution during the processing stage. The gating process permanently alters a significant portion of the atoms that are in their excited states after the first two pulses such that they can no longer decay to their initial ground state. This can be accomplished by illuminating the material with an optical pulse resonant with a transition from the excited state to another state which decays into a metastable state other than the initial ground state. The gating photons could be of sufficient energy to photoionize the excited absorbers and, thus, permanently alter their energy level structure. The electron from the photoionized absorbers could be trapped by an acceptor ion present in the material. Such a process has been demonstrated for holes burned into an inhomogeneous line.[12] Other possible gating methods include two-step photodissociation and two-step donor-acceptor electron transfer.[5] If the gating process is inefficient, it can be repeated until a sufficient ground state population grating is achieved. An example of the timing of the programming and gating pulses is shown in figure 2a.

For applications requiring temporary processing for a time duration much longer than the upper state lifetime but short compared to the ground state storage time, it may not be necessary to gate the absorbers. A single photon storage process could be used. Materials that have multiple ground states (i.e. hyperfine split ground states) can store population gratings by having a percentage of the excited state absorbers decay to a level other than the original ground state. In ground states with nuclear hyperfine splittings, these population gratings can persist for days at liquid helium temperatures.[4,13] These materials have two disadvantages. The first is that the processing stage is destructive. The third laser pulse continually excites the ground state atoms which can then decay to another state depleting the stored population grating. The available processing time is thus limited by the branching ratio of the excited state and the excitation rate required to obtain a satisfactory signal to noise ratio. The second disadvantage is that the ground state splitting may be smaller than the width of the inhomogeneous line. For example, nuclear hyperfine splittings are on the order of tens of megahertz and inhomogeneous linewidths are on the order of several gigahertz. Level overlap will lead to coherent beating and undesired modulation of the output signal. The data bandwidth would be severely limited by the smallest ground state splitting. In this paper, only gated coherent transient processors will be analyzed.

2.2 The Processing Stage

The gating of the material after the first two pulses allows non-destructive probing of the processor by an uninterrupted modulated input signal. The response of the material to this continuous input signal is similar to the response due to the third data pulse in the previously mentioned triple product correlator. The resultant output signal represents the continuous convolution of the input signal with the cross-correlation of the temporal waveforms of the first and second pulses (see figure 2b). There are no restrictions on the duration of the third input signal provided all the excited absorbers relax to the previous ground states (Though the input signal has an indefinite duration with an indefinite number of breaks, it will often be referred to as the third pulse throughout the remainder of this paper). Multi-photon processes may eventually lead to degradation of the stored information and thus impose limits on the third input pulse. Since the processor can accept data continuously, the latency time if not reprogrammed is zero. The propagation delay through the processor is roughly the sum of the durations of the two programming pulses.

To achieve high fidelity output signals, the intensity of the third pulse must be reduced to a level where saturation effects are negligible. Output direction is $\vec{k}_s = \vec{k}_3 + \vec{k}_2 - \vec{k}_1$, where $\vec{k}_1$, $\vec{k}_2$, $\vec{k}_3$, and $\vec{k}_s$ are the wavevectors for the first, second, and third pulses and the output signal, respectively. The output is optimized when the phase matching condition, $|\vec{k}_s| = |\vec{k}_2|$, is satisfied. Since the material is preprogrammed by pulses 1 and 2, during the processing state the output signal need only be isolated from the third pulse. This can be accomplished by introducing slight angular separation between the two programming pulses (as illustrated in figure 1) or by having the pulses be counter-propagating. Large angles are avoided due to beam overlap considerations, not phase matching constraints.

2.3 Reprogramming the Processor

There are two potential methods for reprogramming the processor. The old pattern information could be erased via a reversible gating process and a new pattern programmed into the same spatial volume. In the second method, an 2-D spatial array of patterns is stored in the material. Different patterns are randomly accessed spatially. Access times of a few microseconds could be achieved with acousto-optic or electro-optic deflectors. The pattern storage densities are calculated below and can exceed 10^5 patterns per cm^2. Therefore, in most cases there would be no need to

introduce the two new programming pulses (pulses 1 and 2). This greatly reduces the complexity of the processing stage and reduces the latency time during reprogramming, since the material basically acts as an array of passive filters.

3.0 Analysis of Processor's Performance

The following is an analysis of the performance of a continuous optical processor in the case where the medium is gated after the second pulse. The effects of homogenous and inhomogeneous broadening, coherent and incoherent saturation, output efficiency, shot noise, spatial crosstalk, diffraction, and local heating are considered in evaluating the processor's performance. A method for obtaining optimal performance is prescribed and an example is given. The determination of the maximum achievable time-bandwidth products, processing bandwidths, and storage densities requires the following input parameters: the wavelength, Einstein coefficient, inhomogeneous bandwidth, and homogeneous bandwidth of the absorbing transition; the absorption length and index of refraction of the material; the maximum permissible levels of distortions and crosstalk; the gating and detection efficiency; and the desired number of photoelectons generated by the peak of the output signal. Determining the performance also requires limits to be placed on the intensities of the input signal and the pattern pulse and on the characteristics of their power spectrums. These parameters and limits are defined and discussed below

3.1 Assumptions

For convenience, assume 1) the inhomogeneously broadened absorber has a uniform spectral density of absorbers over the inhomogeneous bandwidth, $\Delta\nu_i$, which is centered around $\nu = c/\lambda$ where λ is the wavelength of the light pulses' optical carrier. 2) the inhomogeneous bandwidth is much greater than the homogeneous bandwidth, $\Delta\nu_h$, 3) the spectrum of the uninterrupted data stream has a bandwidth less than or equal to $\Delta\nu_d$, defined as the processor's data bandwidth, 4) the data stream has the limitation that, averaged over any given time interval, its dynamic power spectrum has the characteristic that the maximum power of any frequency component is less than some specified constant times the average power of the data stream, and 5) the intensity of the data stream averaged over a time interval equal to the dephasing time of the absorbing transition is fairly constant. Making these assumptions greatly simplifies the analysis while introducing only a small error with respect to a model that takes into account the true shape of the inhomogeneous line and data stream's spectrum. When the specific material and data stream

properties are known, the required modifications are straightforward.

The absorption coefficient for a flat inhomogeneously broadened line with an inhomogeneous bandwidth, $\Delta\nu_i$, is given by

$$\alpha = \frac{N \lambda^2 \mathcal{A}_{10}}{8\pi n^2 \Delta\nu_i} \quad , \tag{2}$$

where N is the concentration of absorbers in the material, $\mathcal{A}_{10}$ is the Einstein coefficient for the transition from the ground (level 0) to excited (level 1) state, λ is the vacuum wavelength of the transition, and n is the index of refraction of the host material.

3.2 Coherent Saturation

Assume the medium responds to first order as a non-magnetic, linear medium. The intensity $I_d(t)$ and electric field real amplitude $E_d(t)$ of the continuous third data pulse are related by

$$I_d(t) = \frac{cn \left\langle |E_d(t)|^2 \right\rangle_{\delta t}}{4\pi} \quad , \tag{3}$$

where c is the speed of light in a vacuum and $\langle \ \rangle_{\delta t}$ represents the average of the enclosed function over a time interval δt. The time interval δt is long with respect to an optical period, but short with respect to the reciprocal of the the data bandwidth. The effects of coherent saturation can be evaluated by calculating the extent to which the absorbers are coherently driven in a time period equal to the excitation transition's homogeneous dephasing time, $T_2 = 1/(\pi \Delta\nu_h)$. The Fourier component of the electric field amplitudes at time t taken over a time interval T_2 is defined as

$$\tilde{E}_d(\nu) \equiv \int_{t - T_2/2}^{t + T_2/2} dt' \, E_d(t') \, exp(-i2\pi\nu t) \quad . \tag{4}$$

$\tilde{E}_d(\nu)$ is double peaked with each peak grouped about the positive and negative optical carrier frequency ($\pm c/\lambda$), respectively. It should be noted that since there is no assumption that $E_d(t)$ is repetitive, $\tilde{E}_d(\nu)$ is a time varying quantity and is thus referred to as a dynamic Fourier component. Since $E_d(t)$ is real, $\tilde{E}_d(-\nu) = \tilde{E}_d^*(\nu)$. In accordance with our fourth assumption in section 3.1, define γ_c to be the ratio of the maximum allowable magnitude squared of the dynamic Fourier components to the average magnitude squared of the Fourier components, such that at any given time, t,

$$\gamma_c \geq \frac{Max\left[\left|\tilde{E}_d(\nu)\right|^2\right]}{\left\langle\left|\tilde{E}_d(\nu)\right|^2\right\rangle_{\Delta\nu_d}} , \tag{5}$$

where $\langle\ \rangle_{\Delta\nu_d}$ represents the frequency average over $\Delta\nu_d$. The average is taken only around the positive carrier frequency. Let $\bar{I}_d$ be defined as the maximum intensity of the data stream when averaged over any time interval T_2. Equation (5) and $\bar{I}_d$ are limits of the characteristics of the data signal that must be met to obtain the performance predicted below. Assuming that the power in the data stream outside the data bandwidth is negligible, Parseval's theorem yields

$$\left\langle\left|\tilde{E}_d(\nu)\right|^2\right\rangle_{\Delta\nu_d} = \frac{T_2}{2\Delta\nu_d}\left\langle\left|E_d(t)\right|^2\right\rangle_{T_2} \leq \frac{2\pi\ T_2\ \bar{I}_d}{nc\Delta\nu_d} . \tag{6}$$

The maximum pulse area at time t at a given frequency over the time interval T_2 is given by[14]

$$\theta_{max}(t) = \frac{4\pi p\ Max\left[\left|\tilde{E}_d(\nu)\right|\right]}{h} = \frac{4\pi p}{h}\sqrt{\frac{2\pi\ \gamma_c\ T_2\ \bar{I}_d}{nc\Delta\nu_d}} \leq \theta_l , \tag{7}$$

where θ_l is defined as the maximum data pulse area seen at any frequency and at any time over a time interval T_2,

$$p = \frac{\sqrt{3A_{10}\ h\ \lambda^3}}{8\pi^2} \tag{8}$$

is the dipole moment, and h is Planck's constant. It is assumed that the unit vectors of the dipole moment and electric field are aligned. The maximum allowable photon flux of the continuous third data pulse, F_c, is

$$F_c \equiv \frac{\lambda\bar{I}_d}{hc} \leq \frac{2\pi\ \theta_l^2\ n\Delta\nu_d}{3\gamma_c\ A_{10}T_2\lambda^2} . \tag{9}$$

By establishing an acceptable level of non-linearity in the medium's response to the electric field amplitudes, the value of the maximum allowable pulse area can be set. At the onset of coherent saturation, the medium's response to the peak components in the data pulse's spectrum is no longer linear, but is roughly proportional to the $\sin(\theta_{max})$. To first order, the non-linearity ε is roughly given by

$$\varepsilon \approx \frac{\theta_l}{\sin(\theta_l)} - 1 . \tag{10}$$

If $\varepsilon << 1$, then $\theta_l \approx \sqrt{6\varepsilon}$. The acceptable value of ε, and thus θ_l, will depend on the application requirements. For example, if 10% non-linearity is acceptable, the maximum allowable pulse area is approximately $\pi/4$.

3.3 Incoherent Saturation

Since the duration of the third pulse can be much longer than the homogeneous decay time of the excitation transition, incoherent saturation of the transition must be considered. The coherent transient output signal's electric field amplitude is proportional to the population difference between the ground state (level 0) and excited state (level 1). Take the general case where the decay from level 1 to level 0 has a bottleneck, which will be labeled level 2. Assumption (5) above assumes the dynamic power spectrum of the continuous third pulse when averaged over the effective decay time of upper state population is roughly uniform over the data bandwidth. The effective decay time of the upper state, τ', is discussed below. Define γ_i to be the maximum allowable ratio of the peak value of the time averaged power spectrum to the average value of the time averaged power spectrum. More precisely

$$\gamma_i \geq \frac{Max\left[\left\langle\left|\tilde{E}_d(\nu)\right|^2\right\rangle_\tau\right]}{\left\langle\left\langle\left|\tilde{E}_d(\nu)\right|^2\right\rangle_{\tau'}\right\rangle_{\Delta\nu_d}} \tag{11}$$

at any given time t. This is a further limit on the characteristics of the input data signal. The time-varying induced transition rate, R, between levels 0 and 1 at the peak of the power spectrum is thus governed by

$$R \leq \frac{\gamma_i \alpha \, \Delta\nu_i \, F_d}{N \, \Delta\nu_d} \equiv R_{max} \, , \tag{12}$$

where F_d is the incident photon flux of the continuous third pulse averaged over τ'. If the effective population decay time is sufficiently greater than the coherence decay time T_2 and the peaks in the power spectrum are randomly distributed, then $\gamma_i \approx 1$. If the effective decay time is comparable to the coherence decay time or if there are peaks in the power spectrum that do not average out over time, then γ_i can be as large as γ_c.

Define τ_{10}, τ_{12}, and τ_{20} as the decay times from levels 1 to 0, 1 to 2, and 2 to 0, respectively. By solving the rate equations, the maximum population difference is found to be proportional to

$$\frac{1}{1 + 2R_{max}\tau'} \, , \tag{13}$$

where τ' is the effective decay time of level 1 and is given by

$$\tau' = \frac{\tau_{10}}{2}\left(\frac{\tau_{20} + 2\tau_{12}}{\tau_{12} + \tau_{10}}\right) . \tag{14}$$

The values of τ' under various limits are:

$$\text{For } \tau_{10} << \tau_{12} \text{ and } \tau_{20} << \tau_{12},\ \tau' \approx \tau_{10}. \tag{15}$$

$$\text{For } \tau_{10} << \tau_{12} \text{ and } \tau_{20} >> \tau_{12},\ \tau' \approx (\tau_{10}\tau_{20})/(2\tau_{12}). \tag{16}$$

$$\text{For } \tau_{10} >> \tau_{12} \text{ and } \tau_{20} << \tau_{12},\ \tau' \approx \tau_{12}. \tag{17}$$

$$\text{For } \tau_{10} >> \tau_{12} \text{ and } \tau_{20} >> \tau_{12},\ \tau' \approx \tau_{20}/2 \ . \tag{18}$$

In the section on coherent saturation, an acceptable level of nonlinearity for the processor, ε, was introduced. The non-linearity due to incoherent saturation is roughly equal to the deviation of equation (13) from unity or approximately $2R\tau'$ for $2R\tau' << 1$. In order that incoherent saturation does not introduce non-linearities greater than ε, the condition $2R\tau' \leq \varepsilon$ must hold. Thus, the maximum photon flux of the continuous third pulse limited by incoherent saturation is given by

$$F_i = \frac{4\pi n^2 \Delta\nu_d \varepsilon}{\lambda^2 \mathcal{A}_{10} \tau' \gamma_i} \ . \tag{19}$$

Here (and throughout the paper) it is assumed that the non-linearities due to different effects are uncorrelated, though further study is needed to determine the extent to which this is true. In order to minimize both coherent and incoherent saturation, the maximum allowable photon flux of the continuous third pulse must be less than or equal to the minimum of F_c in equation (9) and F_i in equation (19). In accordance with assumption (5), the time average of the intensity over an interval T_2 is roughly equal to the time average over an interval τ'. If the coherence decay time were a fixed property of the material but the population decay time was variable (i.e. by optical pumping of the bottleneck state to a short lived state), the optimal effective decay time is obtained by setting $F_d = F_i = F_c$, which yields

$$\tau' = \left(\frac{6\, n\, \gamma_c \varepsilon}{\gamma_i \theta_l^2}\right) T_2 \ . \tag{20}$$

Shorter decay times lead to less saturation, but may lower gating efficiencies since in the programming stage there is less time to gate the excited absorbers.

3.4 Output Signal Efficiency

Define the peak output efficiency, η_{peak}, as the ratio of the intensity of the output autocorrelation peaks to the average intensity of the continuous third pulse. The dependence of η_{peak} on 1) the gating efficiency, 2) the properties of the stored pattern pulses, 3) the

homogeneous decay time, 4) the gain efficiency of the material, and 5) the spatial profile of the input beams are discussed below.

Gating efficiency

Define the gating efficiency η_{gate} as the ratio of the number of absorbers that are permanently altered (i.e. photoionized) by the gating pulse to the number of absorbers that were in the excited state just before the gating pulse (for accumulated population gratings, replace η_{gate} with an appropriate accumulated grating efficiency). The output signal electric field amplitude is proportional to the population difference at the time of recall and thus proportional to η_{gate} . The maximum obtainable electric field of a gated coherent transient (when $\eta_{gate} = 1$) is down by a factor of 2 from that of a non-gated coherent transient due to the elimination of the excited state population grating which contains half of the information after the second pulse.[14] The output signal's electric field is equal to $\eta_{gate}/2$ times that of a non-gated coherent transient.

Pattern Pulse Efficiency

To calculate the intensity of the output signal, a particular processor configuration must be chosen. The case considered below is one in which a single pattern pulse is programmed during the programming stage. Assume the second pulse consists of a single subpulse with pulse area equal to θ_2. Let the first pulse be a pattern pulse of total duration τ_{pat}. The electric field of the output signal in the limit of an optically thin sample ($\alpha L << 1$) is given by[14]

$E_s(t) =$

$$\eta_{gate}\ \alpha L\ \sin(\theta_2)\ \frac{\pi p}{h} \int_{-\tau_{pat}/2}^{+\tau_{pat}/2} d\tau\ E_{pat}(\tau)\ E_d(\tau + t - \tau_{21})\ exp(-2(\tau_{21} - \tau)/T_2) \quad , \quad (21)$$

where L is the interaction length in the material, $E_{pat}(t)$ is the real electric field of the pattern (first) pulse, and τ_{21} is the temporal separation between pulses one and two. The time origin $t = 0$ is defined such that $E_{pat}(t)$ is nonzero only from $t = -\tau_{pat}/2$ to $t = +\tau_{pat}/2$. Assuming pulse two immediately follows the pattern pulse, then $\tau_{21} \approx \tau_{pat}/2$. The third pulse $E_d(t)$ can start at any time after the material has been programmed and gated. The exponential term in the integral takes into account the effects of homogeneous coherence decay.

Assume that, over a time interval τ_{pat} about time t', the third pulse matches the first pattern pulse, i.e.

$$E_d(t' + \tau) = \sqrt{\frac{\langle I_d(t' + \tau)\rangle_{\tau_{pat}}}{\langle I_{pat}(\tau)\rangle_{\tau_{pat}}}}\, E_{pat}(\tau) \approx \sqrt{\frac{\bar{I}_d}{\langle I_{pat}(\tau)\rangle_{\tau_{pat}}}}\, E_{pat}(\tau) \ , \qquad (22)$$

where it is assumed that the intensity of the third pulse when averaged over τ_{pat} is roughly equal to $\bar{I}_d$. This assumption is valid if (1) τ_{pat} is not significantly less than T_2, (2) τ_{pat} is much greater than $1/\Delta_d$ and (3) the average intensity of the third pulse is relatively constant. The maximum allowable intensity of the first pulse $\langle I_{pat}(\tau)\rangle_{\tau_{pat}}$ is governed by coherent saturation and is equivalent to the expression in equation (9) if T_2 is replaced with τ_{pat} and γ_c is replaced with γ_c^{pat}. The new parameter γ_c^{pat} is introduced to allow for the case when the spectral characteristics of the pattern pulse differ significantly from those of the continuous pulse three. If the exponential decay term is temporarily ignored, the intensity of the output signal *without homogeneous decay* at the correlation peak is

$$\lim_{T_2 \to \infty} [I_s(t')] \approx \eta_{gate}^2 (\alpha L)^2 \sin^2(\theta_2) \frac{\theta_l^2\, \tau_{pat}\, \Delta\nu_d}{16\gamma_c^{pat}} \bar{I}_d \ . \qquad (23)$$

Note that the intensity of the output peak is proportional to the product $\tau_{pat}\, \Delta\nu_d$, the time-bandwidth product of the processor.

Homogeneous Decay Efficiency

The effect of homogeneous decay on the correlator's operation is to put less weight on the start of the pattern than on the end of it and to reduce the output efficiency. The maximum field non-linearity due to the homogeneous decay is $(1 - exp(-2\tau_{pat}/T_2))$.[14] By bounding this value with the acceptable non-linearity ε, a maximum value for τ_{pat} can be obtained. For $\varepsilon << 1$, the constraint on the ratio of τ_{pat}/T_2 is

$$\beta_{pat} \equiv (\tau_{pat}/T_2) \leq (\varepsilon/2) \ . \qquad (24)$$

To estimate the reduction in the autocorrelation peak intensity due to homogeneous decay, let $|E_{pat}(t)|$ be roughly constant (as in the case of phase modulated input pulses), so that the electric fields can be taken out of the integral in equation (21). The resultant efficiency due to homogeneous decay is

$$\eta_{decay} \equiv \frac{[I_s(t')]}{\lim_{T_2 \to \infty} [I_s(t')]} \approx \left(\frac{1 - exp(-2\beta_{pat})}{2\beta_{pat}}\right)^2 \ , \qquad (25)$$

where the above condition that $\tau_{21} \approx \tau_{pat}/2$ is assumed. It should be noted that the effects of

homogeneous decay can be cancelled by introducing an exponential ramp, $\exp(-4\tau/T_2)$, into the pattern pulse. This would allow $\tau_{pat} \geq T_2$. However, this would require higher complexity in the input devices as well as confidence in the consistency of the homogenous decay rate and in the shape of the decay. For now, assume that the pattern pulse is uncorrected for homogeneous decay.

Gain Efficiency

In an optically thick medium (αL approaching or exceeding unity), the term $(\alpha L)^2$ in equation (23) must be replaced by the gain efficiency of the material, $\eta_{\alpha L}$, which is a non-linear function of αL. For optically thin samples ($\alpha L << 1$), $\eta_{\alpha L} = (\alpha L)^2$.[14] For optically thick samples, the optimal gain efficiency is a balance between the number of radiating absorbers and the absorption of the input pulses and output signal. Consider the case of a stimulated photon echo in which all three excitation pulses are assumed to undergo linear absorption and the polarization is assumed proportional to the cube of the excitation pulse electric fields. It has previously been shown that [14]

$$\eta_{\alpha L} = \left(1 - exp(-\alpha L)\right)^2 exp(-\alpha L) \ . \tag{26}$$

The assumption that all the pulses undergo linear absorption slightly underestimates the gain efficiency since one of the excitation pulses is generally a $\pi/2$ pulse which saturates the medium and the absorber's response to the excitation pulses is not linear but sinusoidal in nature.

Beam Overlap Efficiency

From equations (23), (25), and (26), an expression for the peak output intensity efficiency, η_{peak}, is obtained:

$$\eta_{peak} \equiv \frac{I_s(t')}{\bar{I}_d} \approx \frac{\eta_{gate}^2 \, \eta_{\alpha L} \, \eta_{decay} \, \theta_l^2 \, \tau_{pat} \, \Delta\nu_d}{16 \gamma_c^{pat}} \ . \tag{27}$$

where is is assumed that $\theta_2 = \pi/2$ and that $\langle I_{pat}(\tau) \rangle_{\tau_{pat}}$ equals its maximum allowable value. For gaussian beams, this peak efficiency is only obtained near the center of the beams. As the intensity decreases on the wings of the gaussian, so does the efficiency. If the spatial intensity profile of the j^{th} pulse can be written as

$$I_j(r) = I_j(0) \ exp\left(-\left(\frac{r}{\sigma}\right)^2\right) \ . \tag{28}$$

where r is the radial distance from the center of the gaussian beam, then the integrated power of

the j[th] pulse, P_j, is $\pi\sigma^2 I_j(0)$. The output intensity as a function of radial position for a coherent transient where the second pulse is a brief pulse and the first and third pulses are in the linear regime is given by

$$I_s(r) = \eta_{peak} \quad I_d(r) \frac{I_{pat}(r)}{I_{pat}(0)} \sin^2\left(\theta_2 \sqrt{\frac{I_2(r)}{I_2(0)}}\right) . \tag{29}$$

The total output signal power is the spatial integral of $I_s(r)$. Define the overlap efficiency, $\eta_{overlap}$, as the ratio of the actual output signal power P_s to the ideal output signal power, which is $\eta_{peak} P_d$ (i.e. $P_s = \eta_{overlap}\eta_{peak} P_d$). Efficiencies approaching $\eta_{overlap} = 1$ can be obtained if variable beam widths or non-diffraction limited "top hat" beams are used. However, these techniques lead to increased spatial crosstalk or increased diffraction and, thus, lower pattern densities. In this paper, only gaussian beams of equal width are considered. The overlap efficiency is then

$$\eta_{overlap} = \frac{2}{\sigma^2} \int_0^\infty dr \; r \; \frac{I_d(r)}{I_d(0)} \frac{I_{pat}(r)}{I_{pat}(0)} \sin^2\left(\theta_2 \sqrt{\frac{I_2(r)}{I_2(0)}}\right) . \tag{30}$$

Equation (30) can be numerically integrated. For $\theta_2 = \pi/2$, the result is $\eta_{overlap} = 0.43$. This compares to $\eta_{overlap} = 0.5$ if the sine term were ignored (set to one). By slightly increasing the peak pulse area of pulse two, the overlap efficiency can be optimized to $\eta_{overlap} = 0.46$ when θ_2 equals $(0.59)\pi$.

3.5 Required spot size for shot noise limited detection

Define the detection efficiency η_{det} as the ratio of photons detected to the photons that are emitted in the output signal. Output coupling and scattering losses, as well as the detector's quantum efficiency, are incorporated into the detection efficiency. The number of detected photons, ρ, in a correlation peak is roughly

$$\rho = \left(\frac{\lambda}{hc\Delta\nu_d}\right) \eta_{det} \; \eta_{overlap}\eta_{peak}\pi\sigma^2\bar{I}_d \tag{31}$$

assuming the width of the correlation peak is roughly $1/\Delta\nu_d$. Assuming $\bar{I}_d$ is roughly equal to its maximum value given by equation (9), solving for σ^2 yields

$$\sigma^2 \approx \left(\frac{2^6 \, 3 \, n \, \rho \, \gamma_c^{pat}\gamma_c}{\pi \, \eta_{det} \, \eta_{gate}^2 \, \eta_{overlap} \, \eta_{decay}\theta_l^4}\right)\left(\frac{T_2 \, \Delta\nu_i}{\tau_{pat} \, \Delta\nu_d}\right)\left(\frac{\alpha}{\eta_{cd}}\right)\left(\frac{1}{N}\right) \tag{32}$$

3.6 Pattern Storage Density

The crosstalk from neighboring spots when the third pulse is incident on a given spatial location is now calculated for the cases in which the nearest neighbors have correlated and uncorrelated patterns and for the case where a detection aperture is introduced.

Pattern Storage Density for Uncorrelated Nearest Neighbors

Consider two adjacent storage spots. Define an x-y coordinate system such that the two spots lie on the x-axis separated by x_s with the third pulse centered at the origin. We will ignore the saturation of the second pulse that occurs when writing the adjacent spot. This leads to an overestimate of the crosstalk signal by at most θ_2^2; the error is greatest in the region around the adjacent spot and is negligible in the region around the desired spot. The estimated peak power of the crosstalk signal from a single adjacent spot is

$$P_c(x_s) = \int_{-\infty}^{+\infty} dx \int_{-\infty}^{+\infty} dy \; \eta_{peak} \, \theta_2^2 \, \frac{I_{pat}(x-x_s,y)}{I_{pat}(0)} \, \frac{I_2(x-x_s,y)}{I_2(0)} \, I_d(x,y) \; . \qquad (33)$$

This calculation does not take into account interference between the crosstalk signal and the desired output signal. It assumes that the adjacent spots will have roughly orthogonal patterns stored in them and, therefore, the correlation peaks in the crosstalk signal and the desired output signal will not overlap temporally and coherently interfere. It is also assumed that all the patterns in the adjacent spots are roughly mutually orthogonal so that the peak level of the total crosstalk signal is just the peak level calculated above for a single adjacent spot. For gaussian pulses, the ratio of the crosstalk signal to the desired signal is

$$\frac{P_c}{P_s} = \frac{\theta_2^2}{3\eta_{overlap}} \exp\left(-\frac{2}{3}\left(\frac{x_s}{\sigma}\right)^2\right) . \qquad (34)$$

The maximum pattern density is the reciprocal of the unit cell area which depends on the two dimensional packing geometry. Assuming hexagonal packing, the maximum pattern density for uncorrelated adjacent patterns is

$$D_{max} = \frac{4}{\sqrt{3}x_s^2} = \frac{8}{3\sqrt{3}\sigma^2 \ln\left(\frac{\theta_2^2}{3\eta_{overlap}} \frac{P_s}{P_c}\right)} . \qquad (35)$$

The results are illustrated in trace a of figure 3 for $\theta_2 = (0.59)\pi$ and $\eta_{overlap} = 0.46$. In the figure

the normalized pattern density is defined as $D_{max}\sigma^2$.

Pattern Storage Density for Correlated Nearest Neighbors

If the patterns in the adjacent spots are correlated, the autocorrelation peaks temporally overlap the desired signal's peaks and the interference between the crosstalk and desired output signal must be considered. The result depends significantly on the degree of correlation. The worst case is if all six adjacent spots are programmed identically to the central spot, but in phase or 180 degrees out of phase with the desired signal. The magnitude of the change in the output signal power under these conditions is

$$|\Delta P_s(x_s)| =$$

$$12\eta_{peak}\,\theta_2^2 \int_{-\infty}^{+\infty} dx \int_{-\infty}^{+\infty} dy \; \frac{\sqrt{I_{pat}(x-x_s,y)\; I_{pat}(x,y)\; I_2(x-x_s,y)\; I_2(x,y)}}{I_{pat}(0)\; I_2(0)}\, I_d(x,y) \qquad (36)$$

and

$$D_{max} = \frac{4}{\sqrt{3}x_s^2} = \frac{8}{3\sqrt{3}\sigma^2\, ln\left(\frac{4\,\theta_2^2}{\eta_{overlap}\left|\frac{P_s}{\Delta P_s}\right|}\right)} \; . \qquad (37)$$

The results are illustrated in trace b of figure 3. This condition is to be avoided since the achievable pattern densities are significantly lower in the case of correlated nearest neighbors compared to the case of uncorrelated nearest neighbors for equivalent requirements on the signal to noise ratio.

Pattern Storage Density with a Detection Aperture

The isolation between adjacent spots can be significantly improved by placing an aperture in the image plane of the output signal. Since the stored information is produced by the mixing of two gaussian beams, its spatial extent is much less than that of the gaussian third pulse and a majority of the crosstalk signal comes from the region around the adjacent spots rather than from the region of the desired spot. The case where the output signal is reimaged and centered on a square aperture of width x_s can be calculated numerically, using equation (33), by reducing the limits on the integral to $\pm x_s/2$. The overestimate of the crosstalk signal and, thus, the underestimate of the density due to ignoring the saturation of pulse 2 is negligible under these conditions. The results are shown for the case of uncorrelated adjacent patterns in trace c of figure 3.

3.7 Local Heating

One concern with a continuous input beam is the effect of localized heating of the material. This heating would cause the temperature dependent homogeneous line to broaden. Consider the case where the sample is a rod of radius r_0 and length L. Assume the rod is only cooled on its circumference and the ends are effectively insulated. Assume that all the incident power, P_d, is dissipated in the form of heat uniformly along a cylinder of radius σ and length L centered in the rod. The problem is then axially symmetric and the temperature rise at the center of the beam is easily calculated to be

$$\Delta T = \frac{\left(1 + 2\, ln(r_0/\sigma)\right) P_d}{4\, \pi L\, \kappa} , \tag{38}$$

where κ is the thermal conductivity of the material. In the section 4.1, this effect will be shown to be negligible.

4.0 Optimizing the Processor's Performance

Maximizing pattern storage density requires minimizing σ^2. Note that σ^2 is proportional to $(T_2\, \Delta\nu_i)/(\tau_{pat}\, \Delta\nu_d)$. The limit on τ_{pat} is given in equation (24). The limit on $\Delta\nu_d$ is that it must be proportionately smaller than $\Delta\nu_i$ in order to minimize distortions due to bandwidth limitations. For a given maximum acceptable distortion level and assuming that τ_{pat} and $\Delta\nu_d$ are at their limits, the ratios $\Delta\nu_d/\Delta\nu_i \equiv \beta_d$ and $\tau_{pat}/T_2 = \varepsilon/2$ are fixed. Under these conditions, the pattern density is independent of both the inhomogeneous and homogeneous bandwidths of the medium and, thus, independent of the time-bandwidth product, which is governed by the ratio of these bandwidths.

If the expression in equation (26) is used for $\eta_{\alpha L}$, then the minimum of $(\alpha/\eta_{\alpha L})$ is $5.32/L$ and occurs at $\alpha = .523/L$. Thus, σ^2 is inversely proportional to interaction length, L, and is minimized when L is at its maximum. The maximum path length through the sample is limited by diffraction. To determine the maximum acceptable path length through the sample, consider the intensity profile of a focused gaussian beam:

$$I(z,r) = \frac{I(0,0)}{\left(1+\left(\frac{z}{z_0}\right)^2\right)}\, exp\left(\frac{-\, r^2}{\sigma^2\left(1+\left(\frac{z}{z_0}\right)^2\right)}\right) , \tag{39}$$

where z is the distance away from focus and $z_0 = 2\pi\, n\, \sigma^2/\lambda$. At $\pm z_0/2$, the maximum intensity drop on axis is 20% and the maximum beam width is 12% greater than at the focus. If L is larger

than z_0, the beams will not remain in focus through the sample. This will lead to loss in efficiency and increased crosstalk with neighboring spots. Setting $L = z_0$, neglecting the slight divergence of the beam as it traverses the crystal, and solving for σ^2 yields

$$\sigma_{min}^2 = \sqrt{(5.32)\left(\frac{2^5\, 3\, \rho\, \gamma_c^{pat} \gamma_c}{\pi^2\, \eta_{det}\, \eta_{gate}^2\, \eta_{overlap}\, \eta_{decay} \theta_l^4\, \beta_d \beta_{pat}}\right)\left(\frac{\lambda}{N}\right)} \quad . \tag{40}$$

Solving for σ_{min}^2 fixes the value of the absorbing transition Einstein coefficient:

$$A_{10} = 4\, n\, \Delta\nu_i\, (0.523) / (N\, \lambda\, \sigma_{min}^2)^* \quad . \tag{41}$$

Finally, note that by increasing the absorption concentration, N, the pattern density is increased. Unfortunately, increased absorber concentrations increases the rate of intercenter interactions and can lead to faster dephasing rates and spectral diffusion. These deleterious effects often occur for concentrations above $10^{18}/cm^3$.[5] Equation (40) has been derived assuming that the choice of N is independent of all other parameters. However, to obtain the maximum performance in practice, the relationships between maximum N and other parameters (primarily the inhomogeneous and homogeneous bandwidths, the Einstein coefficient, and the gating efficiency) will have to be introduced into equation (32) before minimizing σ^2. These relationships are material dependent and have not been fully characterized. Thus, equation (40) will be used to estimate the maximum pattern density and assumed valid if conservative values for the maximum concentrations are chosen.

4.1 Performance of an Optimized Processor

To estimate the performance of the continuous correlator with optimized material parameters, typical values for the material and system parameters must be assumed. Reasonable material parameters might be $\lambda = 800$ nm, $n = 1.5$, $\Delta\nu_i = 10$ GHz, and $\Delta\nu_h = 5$ kHz ($T_2 = 64$ μsec). The concentration maximum is taken to be 10^{18} absorbers per cubic centimeter to avoid intercenter interactions. Assume $\eta_{det} = 0.75$, $\eta_{overlap} = 0.46$ ($\theta_2 = 0.59\pi$), $\varepsilon = 0.1$, $\eta_{gate} = 0.1$, and $\beta_d = 0.5$. The value of ε requires $\theta_l = .75$ and $\beta_{pat} = 0.05$ and yields $\eta_{decay} = .91$. Values for γ_c and γ_c^{pat} can be estimated by examining the spectrum of random binary sequences. For sequences up to 8192 in length, the ratio of the spectral power maximum to average value seldom exceeds 12. Set $\gamma_c = \gamma_c^{pat} = 16$ to take into account that the patterns and signals are not actually random. Take γ_i to be the geometric mean of its extreme values of 1 and γ_c, i.e. $\gamma_i = 4$. In the shot noise limit, the number of detected photons required to obtain a bit

error rate of 10^{-9} is $\rho = 116$ if a 50% detection threshold is assumed.

The above input parameters yield the result $\sigma_{min} = 15$ μm. Assuming roughly orthogonal (uncorrelated) adjacent patterns and a crosstalk signal to noise ratio of 10 is acceptable, the maximum pattern storage density without a detection aperture is 2.2×10^5 per cm^2. The data bandwidth is 5 GHz and the time-bandwidth product is 16000. The required value of A_{10} is 180 Hz, which corresponds to an oscillator strength of roughly 1.7×10^{-6}. The optimal path length through the crystal is 2.6 mm and the optimal effective decay time of the excited state is 0.41 msec. The maximum input power is 13 μW and the peak output signal power is 0.19 μW. (To obtain shot noise limited detection would require a cooled avalanche photodiode or coherent detection.) Assuming the sample is a cylinder of radius $r_0 = 5$ cm and has a low thermal conductivity of $\kappa = 0.1$ W/K cm, the temperature rise at the center of the beam is 0.7 mK and, thus, local heating effects are negligible.

The above is a reasonable estimate of the potential performance of the correlator with an optimized material assuming reasonable values for the input parameters. Consider the effects of changing one or more of the input parameters has on the predicted optimized performance. The gating efficiency, η_{gate}, could possibly approach 100% or only be limited to less than 1%, which would increase or decrease, respectively, the pattern density by a factor of 10. The value of γ_c and γ_c^{pat} could be made smaller with appropriate coding of the patterns and signals, yielding a slight increase in the pattern density. The performance is highly dependent on the required linearity. A factor of 2 reduction in epsilon and factor of 2 increase in crosstalk signal to noise leads to a factor of 3.2 reduction in pattern density and a factor of 2 reduction in time-bandwidth product. As mentioned before, if the material's homogeneous decay is well characterized, its effects can be cancelled by appropriate tailoring of the pattern pulse. If β_{pat} is increased from 0.05 to 1.0, a 10-fold increase in the time-bandwidth product and a 3-fold increase in the pattern storage density are realized.

The above examples assumed that the processor's free parameters are reoptimized after each change in the input parameters. For non-optimized parameters, equation (32) yields the required spot size for any given configuration.

5.0 Summary

Modern communication, radar, and object recognition systems often rely on performing real

time convolutions of uninterrupted signal waveforms with multiple fixed-pattern waveforms. Electronic, acoustic, and fiber optic correlators are limited by low time-bandwidth product, low bandwidth, or programming difficulties. Coherent transient processing techniques have advantages over existing technologies due to their high bandwidth and large time-bandwidth product and processing density. Coherent transients respond to the input pulses' field amplitudes. This allows phase and/or amplitude encoding of the pattern and input signals. The continuous processing technique presented here has three distinct advantages over previously presented coherent transient processing techniques. First, the continuous data stream does not need to be broken up into overlapping segments which are shorter than the homogeneous decay time and, then, processed separately. Second, once the first two input pulses have programmed the solid, they need not be reentered. This greatly increases the maximum processing speed, allowing real-time processing of continuous data streams with multi-gigahertz bandwidths and with propagation delays only slightly greater than the duration of the programming pulses. Third, different patterns can be stored at multiple locations in the material and accessed randomly. Access rates of tens of microseconds enable fast reprogramming of the processor without having to reintroduce the programming pulses.

7.0 Acknowledgement

The authors gratefully acknowledge the assistance of Rudy L. Prater in verifying the derivations and editing the manuscript. This research is being sponsored by the Air Force Office of Scientific Research (AFSC) under Contract F49620-91-C-0088.

8.0 References

1. T. W. Mossberg, "Time-domain frequency-selective optical data storage," Opt. Lett. **7**, 77 (1982).

2. W. R. Babbitt and T. W. Mossberg, "Time-Domain Frequency-Selective Optical Data Storage in a Solid-State Material," Opt. Comm. **65**, 185 (1988).

3. M. K. Kim and R. Kachru, "Multiple-Bit Long-Term Data Storage by Backward Stimulated Echo," Opt. Lett. **14**, 423 (1989).

4. M. Mitsunaga, R. Yano, and N. Uesugi, "Time- and frequency-domain hybrid optical memory: 1.6-kbit data storage in Eu^{3+}:Y_2SiO_5," Optics Letters **16**, 1890 (1991).

5. W. E. Moerner, "Molecular electronics for frequency domain optical storage: Persistent spectral hole-burning," *J. Molec. Elec.* **1**, 55 (1985); *Frequency domain optical storage and other applications of persistent spectral hole-burning,"* Chapter 7 in Persistent Spectral Hole-Burning: Science and Applications, W. E. Moerner, Ed., Topics in Current Physics Vol. 44, Springer-Verlag, 1988 and references therein.

6. Y. S. Bai, W. R. Babbitt, N. W. Carlson, and T. W. Mossberg, "Real-time optical waveform convolver/cross correlator," Appl. Phys. Lett. **45**, 714 (1984).

7. J. A. Bell and W. R. Babbitt, "Phase and frequency sensitive signal processing using stimulated photon echoes", Conference on Lasers and Electro-Optics, Anaheim, 1990 Technical Digest Series (Optical Society of America, Washington, DC 1990) Vol. 7, pp 420-421.

8. T. W. Mossberg, Y. S. Bai, W. R. Babbitt, and N. W. Carlson, "Optical cross-correlation and convolution apparatus," U. S. Patent No. 4,670,854 (June 2, 1987).

9. W. R. Babbitt and J. A. Bell, "An optical signal processor for processing continuous signal data," U. S. Patent Application Pending.

10. W. R. Babbitt, Y. S. Bai, and T. W. Mossberg, "Convolution, Correlation, and Storage of Optical Data in Inhomogeneously Broadened Materials," *Optical Information Processing II*, P. R. Pape ed., SPIE **639**, Bellingham, Wa. (1986).

11. R.M.Macfarlane and R.M.Shelby, "Sub-kilohertz optical linewidths of the $^7F_0$-$^5D_0$ transition in Y_2O_3:Eu^{3+}," Opt. Commun. **39**, 169 (1981).

12. A. Winnacker, R. M Shelby, and R. M. Macfarlane, "Photon-gated hole burning: a new mechanism using two-step photoionization," Opt. Lett. **10**, 350 (1985).

13. W. R. Babbitt, A. Lezama, and T. W. Mossberg, "Optical Dephasing, Hyperfine Structure, and Hyperfine Relaxation Associated with the 580.8nm $^7F_0$-$^5D_0$ Transition in Eu^{3+}:Y_2O_3,"Phys. Rev. B1 39, 1987 (1989).

14. W. R. Babbitt, The Response of Inhomogeneously Broadened Optical Absorbers to Temporally Complex Light Pulses, PhD Thesis, Harvard University, November 1987.

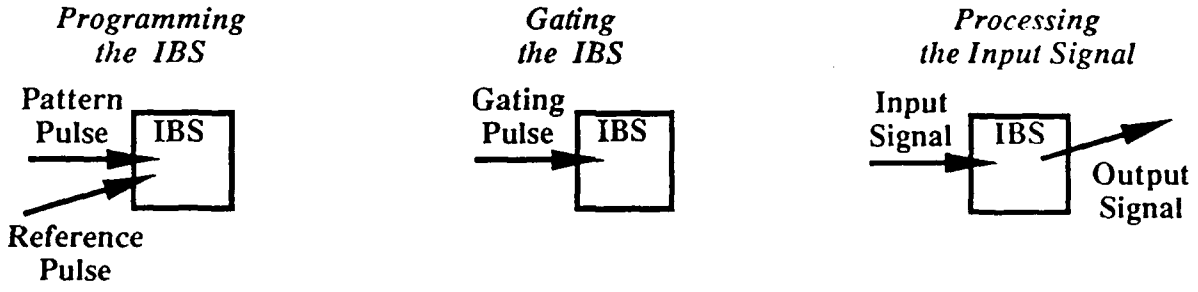

Figure 1. The three steps for signal processing: programming the inhomogeneously broadened solid (IBS), gating the IBS, and processing the continuous input signal. As drawn, the output signal propagates in the same direction as the reference pulse.

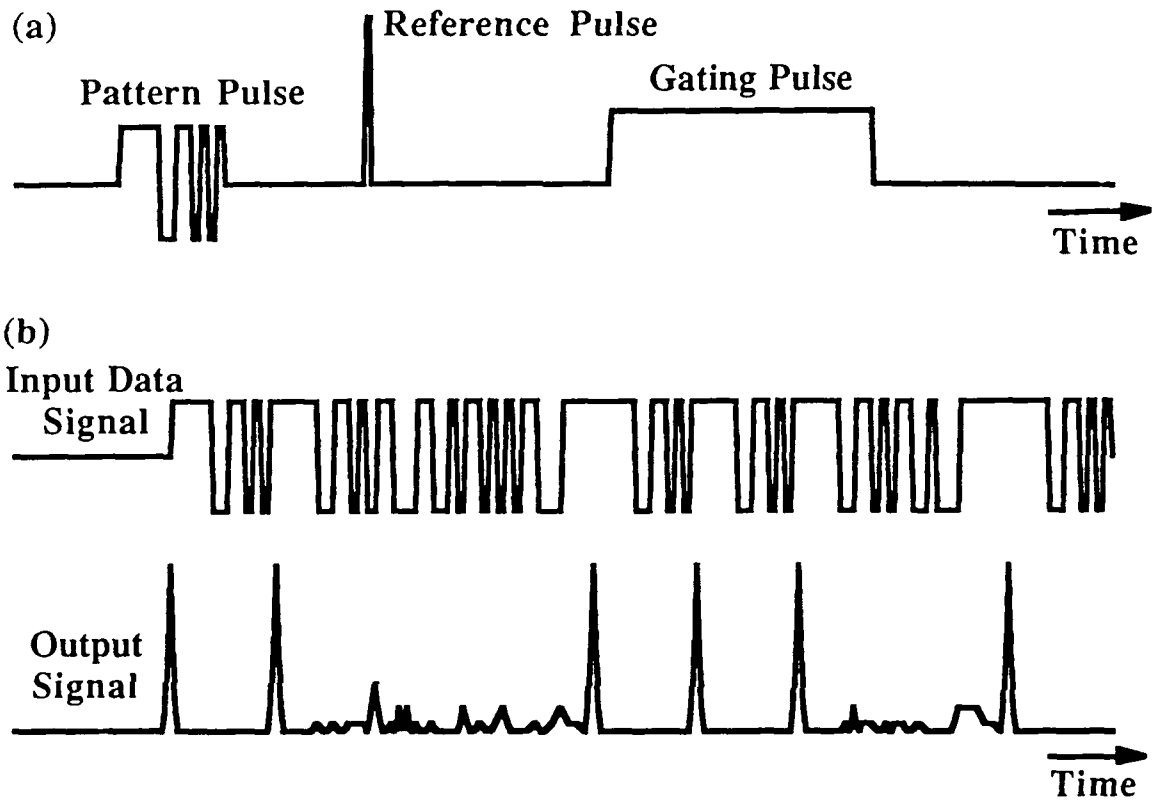

Figure 2. (a) The timing of the programming pulses and the gating pulse. The pattern pulse is a phase encoded 13-bit Barker code. (b) Segments of the continuous input data signal and resultant output signal are shown. The upper trace shows the amplitude of the input signal and the lower trace shows the intensity of the output signal. The input data signal is phase encoded. The 13-bit Barker code use for the pattern pulse is repeated six times in this segment of the input data signal with random bits separating them. The peaks in the output signal intensity correspond to correlations between the pattern pulse and input data signal. The actual output signal will be delayed by the temporal separation between the pattern and reference pulses.

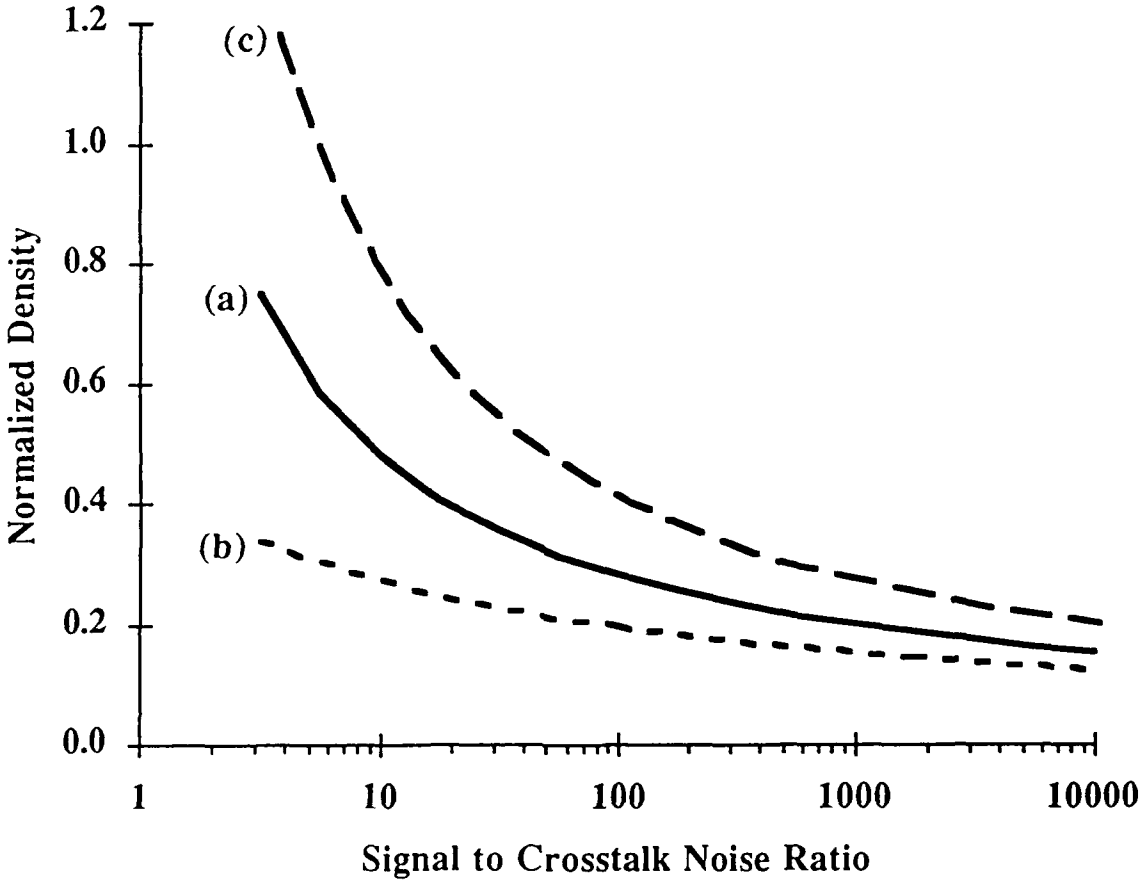

Figure 3: The normalized pattern density versus the signal to crosstalk noise ratio for (a) uncorrelated nearest neighbors and no detection aperture, (b) correlated nearest neighbors and no detection aperture, and (c) uncorrelated neighbors and a square detection aperture.